Oxygen Defects in Phosphorene

A. Ziletti, A. Carvalho, D. K. Campbell, D. F. Coker, and A. H. Castro Neto

Phys. Rev. Lett. **114**, 046801 — Published 28 January 2015

DOI: 10.1103/PhysRevLett.114.046801

Oxygen defects in phosphorene

A. Ziletti,[1] A. Carvalho,[2] D. K. Campbell,[3] D. F. Coker,[1,4] and A. H. Castro Neto[2,3]

[1] *Department of Chemistry, Boston University, 590 Commonwealth Avenue, Boston Massachusetts 02215, USA*
[2] *Centre for Advanced 2D Materials and Graphene Research Centre, National University of Singapore, 6 Science Drive 2, 117546, Singapore*
[3] *Department of Physics, Boston University, 590 Commonwealth Avenue, Boston Massachusetts 02215, USA*
[4] *Freiburg Institute for Advanced Studies (FRIAS), University of Freiburg, D-79104, Freiburg, Germany*

Surface reactions with oxygen are a fundamental cause of the degradation of phosphorene. Using first-principles calculations, we show that for each oxygen atom adsorbed onto phosphorene there is an energy release of about 2 eV. Although the most stable oxygen adsorbed forms are electrically inactive and lead only to minor distortions of the lattice, there are low energy metastable forms which introduce deep donor and/or acceptor levels in the gap. We also propose a mechanism for phosphorene oxidation involving reactive dangling oxygen atoms and we suggest that dangling oxygen atoms increase the hydrophilicity of phosphorene.

PACS numbers: 73.20.At,73.20.Hb

Phosphorene, a single layer of black phosphorus[1, 2], has revealed extraordinary functional properties which make it a promising material not only for exploring novel physical phenomena but also for practical applications. In contrast to graphene, which is a semi-metal, phosphorene is a semiconductor with a quasiparticle band gap of 2 eV. The optical band gap is reduced to 1.2 eV, because of the large exciton binding energy (800 meV)[3, 4]. Phosphorene's peculiar structure of parallel zig-zag rows leads to very anisotropic electron and hole masses, optical absorption and mobility[5–7]. Both its gap and the effective masses can be tuned by stressing phosphorene's naturally pliable waved structure. Strain along the zigzag direction can switch the gap between direct and indirect[8] and compression along the direction perpendicular to the layers can in principle even transform the material into a metal or semimetal[1]. Phosphorene has also scored well as a functional material for two-dimensional electronic and optoelectronic devices. Multi-layer phosphorene field effect transistors have already been demonstrated to exhibit on-off current ratios exceeding 10^5, field-effect mobilities of 1000 cm^2/Vs[9], and fast and broadband photodetection[10].

An invariable issue encountered in the manipulation of phosphorene is the control of the oxidation. The presence of exposed lone pairs at the surface makes phosphorus very reactive to air. Surface oxidation is made apparent by the roughening, which grows exponentially during the first hour after exfoliation[11] and contributes to increasing contact resistance, lower carrier mobility and possibly to the mechanical degradation and breakdown. Thus, identifying the mechanisms of phospherene oxidation – including the electrically active forms of oxygen and how they are introduced – is essential to understanding the real material and its applications.

In this Letter, we show that oxygen chemisorption onto phosphorene is exoenergetic and leads to the formation of neutral defects, as well as to metastable electrically active defect forms. We also discuss the conditions necessary for extensive oxidation and propose strategies to control it.

Oxygen defects were modeled using first-principles calculations based on density functional theory (DFT), as implemented in the QUANTUM ESPRESSO package[12]. Spin-polarized calculations were carried out for triplet states, while singlet states were modeled as closed-shell systems within spin-restricted DFT to avoid spin contamination[13]. We used three different approximations for the exchange-correlation energy: the semilocal generalized gradient approximations PBE[14] and PBEsol[15] functionals, and the HSE06[16] range-separated hybrid functional. The band structures were computed with the PBEsol functional. We validated the binding energies using the PBE and HSE functionals, the former being typically superior to PBEsol for dissociation or cohesive energies[15], and the latter to account for the role of exchange in determining the oxidation states of the oxygen molecule[17]. Unless otherwise stated, all energies reported were obtained with the PBE functional. Activation energies were obtained using the climbing nudged elastic band (NEB) method[18]. Additional computational details are presented in Supplemental Material[19].

Although the fast degradation of black phosphorus when exposed to air[11, 26–29] may involve the reaction with molecules other than oxygen (e.g. water vapor), here we first consider, for simplicity, only the adsorption and incorporation of oxygen. In particular, it is crucial to determine whether O chemisorption is energetically favored or not. To this end, for each oxidized structure we calculate the average binding energy for an oxygen atom, E_b, defined as $E_b = 1/N_{\mathrm{O}} \left[E_{ox} - (E_p + N_{\mathrm{O}} E_{\mathrm{O}_2}/2)\right]$ where N_{O} is the number of O atoms in the cell used in the calculation, E_{ox}, E_p and

E_{O_2} are the total energies of the oxidized phosphorene, the pristine phosphorene, and the O_2 (triplet) molecule, respectively. According to the definition above, a negative E_b indicates that the chemisorption is exothermic (energetically favored).

Chemisorbed or interstitial oxygen atoms can occupy numerous positions in the phosphorene lattice. The most relevant structures are listed on Table I. These are also depicted in Figs. 1-3.

Table I: Binding energies for the isolated oxygen impurities.

Structure	E_b(eV)		
	PBEsol	PBE	HSE
Dangling	-2.22	-2.08	-1.82
Interstitial bridge	-1.77	-1.66	-1.60
Horizontal bridge	-0.21	0.01	0.53
Diagonal bridge	-0.22	0.08	0.75

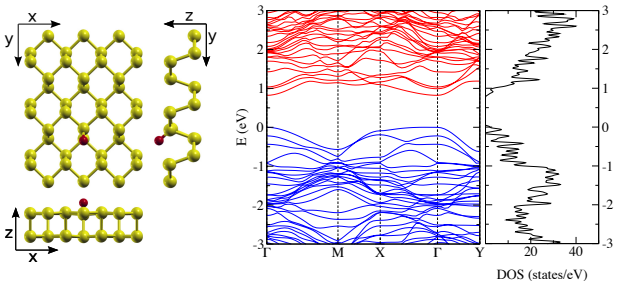

(a) (b)

Figure 1: Dangling oxygen: (a) projections of the structure; (b) electronic band structure (left) and DOS (right). The top of the valence band is set to zero. The band structure of pristine phosphorene is provided in Supplemental Material[19].

The lowest energy structure (highest binding energy) corresponds to an oxygen chemisorbed in a dangling configuration (Fig.1a). The oxygen bonds with one phosphorus atom, with a P-O bond length of 1.50 Å; the bond is short and polar, due to the large difference in electronegativity between P and O (2.19 eV vs 3.44 eV, respectively). Moreover, the P-O bond is tilted by 44.5° away from the phosphorene surface. The phosphorus involved in the P-O bond gets dragged into the lattice by 0.11 Å in the z direction; apart from that, the lattice deformation is minimal. The binding energy is very high, -2.08 eV and -1.82 eV at the PBE and HSE levels, respectively. Thus, the oxygen chemisorption is a strongly exothermic process, with a large energy gain as a result of the formation of the P-O bond, even at the expense of an O=O bond. This defect is electrically neutral, as it introduces no states in the gap (Fig. 1). The DOS (Fig.1b) of the bands close to the Fermi energy is nearly identical to that of pristine phosphorene[19].

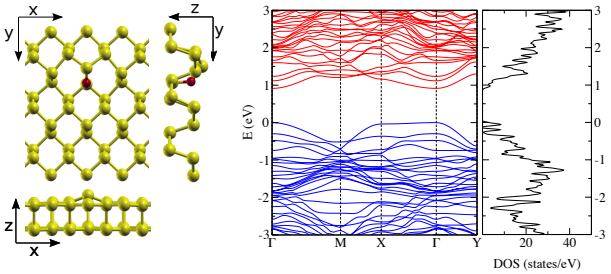

(a) (b)

Figure 2: Interstitial oxygen: (a) projections of the structure; (b) electronic band structure (left) and DOS (right). The top of the valence band is set to zero.

The second lowest energy configuration, which is also electrically neutral, is the interstitial oxygen bridge, shown in Fig.2. In this case, the O penetrates into the lattice, occupying a position close to a P-P bond centre, and forming a bridge between the two P atoms, resembling the structure of interstitial oxygen in silicon[30]. The resulting P-O bond lengths are 1.66 Å and 1.68 Å and the P-O-P bond angle is 129.6°. The oxygen atom pushes one of its P neighbors outwards, as clearly seen in Fig.2a (bottom). The monolayer thickness is now 2.87 Å, which corresponds to an increase of 36% *w.r.t.* pristine phosphorene (2.11 Å). This huge deformation of the structure due to the oxygen bridge is likely to contribute to the carrier scattering and even jeopardize the stability of the crystal, especially for larger impurity concentrations. Despite the large structural change of the lattice, the formation of interstitial oxygen bridges is highly exothermic, with a binding energy of -1.66 eV (-1.60 eV) at the PBE (HSE) level. No states are formed in the middle of the gap (Fig.2b), and the transformation from dangling to interstitial oxygen requires an activation energy of 0.69 eV.

There are other metastable bridge-type surface defects with positive binding energies (Table I), which may be formed if the oxygen source is more reactive than the O_2 ground state (for example, under light pumping).

Two possible configurations are found: the oxygen is on top of the zigzag ridges, and can either form a diagonal bridge[19] – connecting atoms on different edges of the zigzag – or a horizontal bridge (Fig.3a) – connecting atoms from the same edge. Both types of surface bridge defects create levels in the gap.

In the diagonal bridge configuration, the two P-O bonds are identical, with bond length of 1.73 Å and bond angle of 77.0°. The two P atoms involved in the bonding are dragged together by the oxygen bridge and their distance is reduced from 2.21 Å in pristine phosphorene to 2.15 Å. This defect introduces an acceptor state and a perturbed valence band like state[19]. The perturbed va-

lence band state is the result of the hybridization between p_z orbitals of the oxygen and p orbitals of neighboring P atoms, while the acceptor state consists of p_x and p_y orbitals from the O and p orbitals from adjacent P atoms. The strong localization of the perturbed valence band state results in a large peak in the DOS. By comparison, the acceptor state is slightly more dispersive, and thus produces a broader new set of states from 0 to 0.5 eV, just above the Fermi energy.

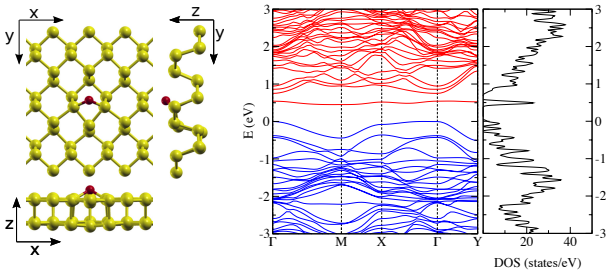

(a) (b)

Figure 3: Horizontal oxygen bridge: (a) projections of the structure; (b) electronic band structure (left) and DOS (right). The top of the valence band is set to zero.

The horizontal bridge defect has similar properties. The P-O bonds are now 1.75 Å long and form an angle of 107.9°. The distance between the P atoms involved in the bonding is 2.83 Å, decreased by 0.45 Å *w.r.t.* pristine phosphorene. This defect introduces a deep acceptor state at 0.5 eV near the conduction band. This mid-gap state is formed by the p_x orbital of the O and the p orbitals of the two P atoms involved in the P-O bonding. In addition, there is also a perturbed valence band state. Such gap states are expected to give rise to recombination lines in luminescence experiments.

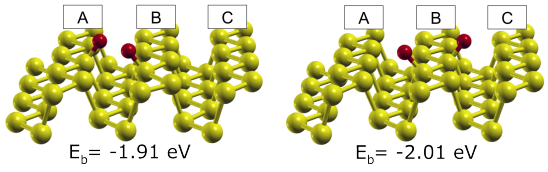

(a) (b)

Figure 4: Possible configurations for two chemisorbed dangling oxygens.

Finally, for the most stable (dangling) configuration, we investigate the interaction of two chemisorbed oxygens. Chemisorbed oxygen atoms repel each other due to the Coloumb interaction between their p orbitals. However, close configurations may be formed kinetically following the dissociation of oxygen molecules. Even though the repulsion between neighboring oxygen atoms (e.g. Fig.4a) reduces the binding energy per O atom of the complex by up to 0.4 eV, the dissociation of O_2 and subsequent formation of two P-O bonds is still very exoenergetic. The oxygen atoms always point away from the zigzag ridge on which they are chemisorbed (labeled as A, B or C in Fig.4), regardless the position of the other oxygen. The interaction between dangling oxygens depends on both distance and relative orientation of their P-O bonds. Configurations in which the oxygens point in different directions (e.g. Fig.4b) are favored *w.r.t.* configurations where they point towards each other (e.g. Fig.4a). For greater distances (>5 Å), the electrostatic interaction between the P-O bond dipoles and the strain interaction fall quickly, resulting in repulsive energies below 0.01 eV. Thus, the chemisorption of oxygen molecules is likely to be a random process, or rather determined by the presence of local impurities or other defects.

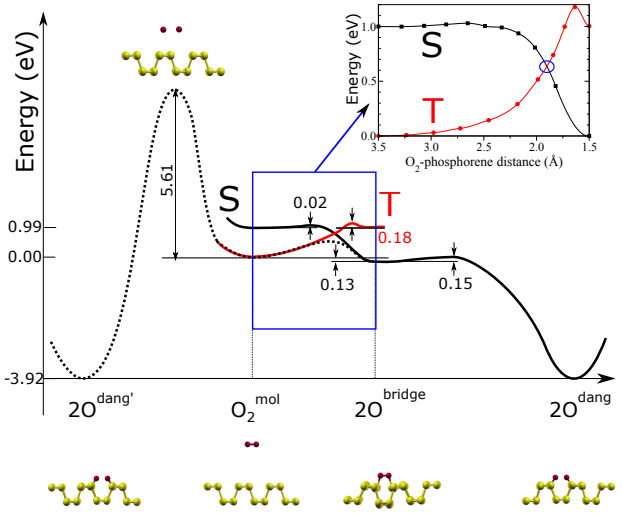

Figure 5: Schematic configuration-coordinate diagram for possible mechanisms for phosphorene oxidation. The solid (dotted) lines indicates the potential energy surfaces (PESs) calculated with fixed (variable) total magnetization. Singlet (black) and triplet (red) PES as a function of the O_2-phosphorene distance are shown in the inset.

In a normal working environment, oxygen is present in its molecular form with its triplet ground state ($^3\Sigma_g^-$), in which the doubly degenerate π_{2p}^* orbitals are each only half filled by two electrons with parallel spin. Our calculations show that dissociation of O_2, and subsequent formation of two dangling oxygens leads to an energy gain of about 4 eV. Further, molecular oxygen can in principle dissociate on the phosphorene surface by either a direct or an indirect mechanism, through intermediate states where one or two oxygen atoms are bound to phosphorene, as shown in Fig.5. Direct dissociation of O_2, however, would require overcoming a barrier of 5.6 eV (Fig.5, left side), close to its binding energy (6.2 eV at the PBE level[31]) and therefore is highly improbable without photo excitation. Consistent with

our findings, an alternative indirect pathway is likely to be the main oxidation channel. Oxygen is initially physisorbed at 3.2 Å parallel to the phosphorene surface with a small binding energy (-0.01 eV and -0.08 eV at the PBE and PBE+vdW[32] level, respectively, see Supplemental Material[19]). The system is in a triplet state, and no charge transfer between O_2 and phosphorene is observed. As the oxygen molecule gets closer to the surface, the degeneracy of its π^*_{2p} orbitals is lifted due to the hybridization with the phosphorene lone pairs, and the singlet state becomes more stable than the triplet. Therefore, there must be at least one point in configuration space where the triplet and singlet potential energy surfaces (PESs) cross, and triplet-to-singlet conversion likely takes place non-radiatively through intersystem crossing (ISC). This crossing occurs when the oxygen molecule is approximately 1.9 Å above the phosphorene surface (see Fig.5-inset). Eventually O_2 is chemisorbed, forming a diagonal molecular bridge, with an energy gain of 0.13 eV *w.r.t.* isolated (triplet) oxygen and pristine phosphorene. This is similar to one of the proposed pathways for oxidation of silicon[33, 34] and graphene [35]. As is clear from the PESs in Fig.5, in the adiabatic approximation, reaching the oxygen molecular bridge configuration requires an activation energy that depends on the crossing point between triplet and singlet PESs. A spin-unrestricted variable-magnetization calculation gives a barrier of 0.54 eV. Once the oxygen bridge has been formed, however, only 0.15 eV is needed for the spin-allowed phonon-mediated dissociation of the O_2 bridge, and subsequent formation of two dangling O, with an energy gain of ∼3.9 eV. The bottleneck of phosphorene oxidation is then the initial chemisorption, where the system needs both to overcome an energy barrier and undergo an ISC, an inherently slow process. Landau-Zener[34, 36, 37] theory provides an estimate of the probability P_{ts} for the (single passage) triplet-to-singlet conversion: $P_{ts} = 2\left[1 - \exp(-V^2/hv\,|F_t - F_s|)\right]$, where V is the spin-orbit matrix element between the triplet and singlet states of free O_2, v is the velocity of an incident O_2 molecule, F_s and F_t are the slopes of the singlet and triplet PES at the crossing point, and h is the Planck's constant. By using $V = 122$ cm^{-1}[34, 37, 38], and estimating v from the O_2 center-of-mass thermal energy at 300 K[35, 37], we obtain $P_{ts} = 0.12$. Thus, the triplet-to-singlet conversion limits this oxidation channel. Nonetheless, due to the small energy barrier and the high exothermicity of the reaction, dangling oxygen defects will be present on the phosphorene surface after exposure to oxygen (or air). Using an attempt frequency $\nu = 10^{13}$ s^{-1}, we estimate a rate of the order of 10^3 s^{-1} at room temperature. In addition, singlet oxygen is expected to readily oxidize phosphorene because only two low barriers (0.02 and 0.15 eV) separate the physisorbed oxygen from the lowest energy chemisorbed configuration.

From these theoretical results, we can infer the effects of oxidation and how they can be detected. The readiness with which phosphorene oxidizes in air is easily explained by the stability of the oxygen defects, which have binding energies of up to -2.1 eV per oxygen atom. However, the formation of surface dangling oxygen defects requires an activation energy of at least ∼0.54 eV leading to the structure shown in Fig. 1(a). This energy has to be provided either thermally or possibly by light-induced excitation of the O_{2p} electrons. The penetration of O into the lattice from the dangling configuration requires an activation energy of 0.69 eV, and probably occurs in a subsequent stage. The most stable oxygen defects are electrically neutral, in analogy with the case of interstitial oxygen in Czocharlski silicon, which in its isolated state leaves the electronic properties unaffected[30]. Dangling oxygen defects cause little lattice deformation. However, they change the surface affinity to interact with other species present in air. Once some oxygen atoms are chemisorbed, the surface will be polarized, due to the difference in electronegativity between O and P, and will become more hydrophilic. The O atoms serve in fact as anchors for hydrogen bonds with water molecules resulting in a binding energy of -0.22 eV, to be compared with -0.09 eV for a water molecule physisorbed onto a bare phosphorene surface[19]. Thus, even though dangling oxygen defects themselves do not change drastically the properties of the material, they can be a starting point for the formation of more complex defects involving water or other polar molecules. The presence of oxygen defects might indeed play a role in the hydrophilicity of few-layer black phosphorus observed after air exposure[29].

Recently it has been claimed[39] that the simultaneous presence of oxygen, water and light is necessary for few-layer black phosphorus oxidation. Our results (Fig.5) show that oxidation should also be possible in pure oxygen atmosphere (under light illumination). The issue seems to be how oxidation is detected. Conventional Raman spectroscopy is sometimes not sensitive to surface-adsorbed species on semiconductors, especially if present at low concentration[40]. Moreover, since the experiment in Ref. [33] was performed on few-layer black phosphorus (not monolayer) the majority of the Raman signal probably comes from the pristine layers underneath the first oxidized layer; P-O vibrational modes might also be hidden beneath the SiO_2 substrate vibrational background. Surface-sensitive spectroscopic techniques, such as surface-enhanced Raman spectroscopy[41] (SERS) or vibrational sum frequency generation[42] (VSFG), may be required for experimental detection and classification of oxygen defects. We found that dangling oxygen gives rise to a local vibrational mode at 1099 cm^{-1}, while interstitial oxygen originates two local vibrational modes at 574 cm^{-1} and 763 cm^{-1}.

For low oxygen concentrations, the activation energy for oxygen insertion (forming interstitial oxygen from an

initial dangling configuration) is W= 0.69 eV. Estimating the transition rate $R = \nu \exp(-W/kT)$ using the typical vibrational attempt frequency $\nu = 10^{13}$ s^{-1}, the transition rate at room temperature is already of the order of 10 s^{-1}. Thus, some interstitial oxygen may be formed at room temperature, albeit at a concentration orders of magnitude lower than dangling oxygen.

Nevertheless, oxygen insertion into the lattice results in considerable deformation, expanding the P-P distance, increasing the local layer thickness by 36%. This promotes further oxidation in the neighborhood of the pre-existing interstitial oxygen defects. Further, for high enough interstitial oxygen concentration, the crystal might break apart due to this large stress, probably forming molecular compounds such as phosphorus trioxide (P_4O_6), phosphorus pentoxide (P_4O_{10}) or phosphates.

Even though oxygen bridge-type defects are metastable, they can be formed under non-equilibrium conditions. Such defects are electrically active, introducing deep acceptor states and perturbed valence states. It is noteworthy that in thicker multilayer black phosphorus (more than three layers), the acceptor state of the diagonal bridge defect hybridises with the valence band[43], and likely contribute to the *p*-type conductivity often observed in samples not intentionally doped[2, 44].

Since the formation of the electrically active defects requires a larger activation energy, a possible strategy to avoid their formation is to process the samples in dark and at low temperature. Further, avoiding the contact of oxidized samples with water may prevent the formation of more complex defects and sample deterioration.

A.Z. and D.F.C. acknowledge NSF grant CHE-1301157 and also an allocation of computational resources from Boston University's Office of Information Technology and Scientific Computing and Visualization. A.Z. also acknowledges the support from grant CMMI-1036460, Banco Santander. A.H.C.N. and A.C. acknowledge the National Research Foundation, Prime Minister's Office, Singapore, under its Medium Sized Centre Programme and CRP award "Novel 2D materials with tailored properties: beyond graphene" (R-144-000-295-281).

[1] A. S. Rodin, A. Carvalho, and A. H. Castro Neto, Phys. Rev. Lett. **112**, 176801 (2014).
[2] H. Liu, A. T. Neal, Z. Zhu, Z. Luo, X. Xu, D. Tomanek, and P. D. Ye, ACS Nano, **8**(4), 4033 (2014).
[3] V. Tran, R. Soklaski, Y. Liang, and L. Yang, Phys. Rev. B **89**, 235319 (2014).
[4] A. S. Rodin, A. Carvalho, and A. H. Castro Neto, Phys. Rev. B **90**, 075429 (2014).
[5] T. Low, A. S. Rodin, A. Carvalho, Y. Jiang, H. Wang, F. Xia, and A. H. Castro Neto, Phys. Rev. B **90**, 075434 (2014).
[6] F. Xia, H. Wang, and Y. Jia, Nat. Commun. **5**, 4458 (2014).
[7] J. Qiao, X. Kong, Z. Hu, F. Yang, and W. Ji, Nat. Commun. **5**, 4475 (2014).
[8] R. Fei, and L. Yang, Nano. Lett. **14**(5), 2884 (2014).
[9] L. Li, Y. Yijun, G. J. Ye, Q. Ge, X. Ou, H. Wu, D. Feng, X. H. Chen, and Y. Zhang, Nat. Nano. **9**, 372 (2014).
[10] M. Buscema, D. J. Groenendijk, S. I. Blanter, G. A. Steele, H. S. J. van der Zant, and A. Castellanos-Gomez, Nano Lett. **14**(6), 3347(2014).
[11] S. P. Koenig, R. A. Doganov, H. Schmidt, A. H. Castro Neto, and B. Ozyilmaz, App. Phys. Lett. **104**(10), 103106(2014).
[12] P. Giannozzi *et al.*, J. Phys. Condens. Matter 21, 395502(2009).
[13] S. P. Chan, G. Chen, X. G. Gong, and Z. F. Liu, Phys. Rev. Lett. **90**, 086403(2003).
[14] J. P. Perdew, K. Burke, and M. Ernzerhof, Phys. Rev. Lett. **77**, 3865(1996).
[15] J. P. Perdew, A. Ruzsinszky, G. I. Csonka, O. A. Vydrov, G. E. Scuseria, L. A. Constantin, X. Zhou, and K. Burke, Phys. Rev. Lett. **100**, 136406(2008).
[16] A. V. Krukau, O. A. Vydrov, A. F. Izmaylov, and G. E. Scuseria, J. Chem. Phys. **125**(22), 224106(2006).
[17] D. Colleoni, and A. Pasquarello, App. Surf. Sci. **291**, 6 (2014).
[18] G. Henkelman and H. Jonsson, J. Chem. Phys. **113**(22), 9978(2000).
[19] See Supplemental Material [url], which includes Refs. [20-25]
[20] P. E. Blochl, Phys. Rev. B **50**, 17953 (1994).
[21] N. Troullier, and J. L. Martins, Phys. Rev. B **43**, 1993 (1991).
[22] H. J. Monkhorst, and J. D. Pack, Phys. Rev. B **13**, 5188 (1976).
[23] P. E. Blochl, O. Jepsen, and O. K. Andersen, Phys. Rev. B **49**, 16223(1994).
[24] S. Baroni, S. de Gironcoli, A. Dal Corso, and P. Giannozzi, Rev. Mod. Phys. **73**, 515(2001).
[25] S. Grimme, J. Comput. Chem. **27** (15), 1787(2006).
[26] J. Brunner, M. Thuler, S. Veprek, and R. Wild, J. Phys. Chem. Solids **40** (12), 967 (1979).
[27] S. Yau, T. P. Moffat, A. J. Bard, Z. Zhang, and M. M. Lerner, Chem. Phys. Lett. **198** (3), 383 (1992).
[28] T. W. Farnsworth, R. A. Wells, A. H. Woomer, J. Hu, C. Donley, and S. C. Warren, IPS14: Informal Phosphorene Symposium, August 2014 (unpublished).
[29] A. Castellanos-Gomez, L. Vicarelli, E. Prada, J. O. Island, K. L. Narasimha-Acharya, S. I. Blanter, D. J. Groenendijk, M. Buscema, G. A. Steele, J. V. Alvarez, H. W. Zandbergen, J. J. Palacios, and H. S. J. van der Zant, 2D Mater. **1**(2), 025001 (2014).
[30] J. Coutinho, R. Jones, P. R. Briddon, and S. Oberg, Phys. Rev. B **62**, 10824(2000).
[31] L. Schimka, J. Harl, and G. Kresse, J. Chem. Phys. **134**(2), 024116(2011).
[32] S. Grimme, J. Comput. Chem. **27** (15), 1787(2006).
[33] X. L. Fan, Y. F. Zhang, W. M. Lau, and Z. F. Liu, Phys. Rev. Lett. **94**, 016101(2005).
[34] K. Kato, T. Uda, and K. Terakura, Phys. Rev. Lett. **80**, 2000(1998).
[35] S. Zhou, and A. Bongiorno, Sci. Rep. **3**, 2484 (2013).

[36] C Zener. Proc. Roy. Soc. London Ser. A **137**, 696(1932).
[37] W. Orellana, A. J. R. da Silva, and A. Fazzio, Phys. Rev. Lett. **90**, 016103(2003).
[38] S. R. Langhoff, J. Chem. Phys. **61**(5), 1708(1974).
[39] A. Favron, E. Gaufres, F. Fossard, P. Levesque, A. Phaneuf-L'Heureux, N. Y-W.Tang, A. Loiseau, R. Leonelli, S. Francoeur, and R. Martel, arXiv: 1408.0345.
[40] L. G. Quagliano, J. Am. Chem. Soc. **126**(23), 7393(2004).
[41] M. Fleischmann, P.J. Hendra, and A.J. McQuillan, Chem. Phys. Lett. **26**(2), 163(1974).
[42] F. Vidal and A. Tadjeddine, Rep. Prog. Phys. **68**(5), 1095(2005).
[43] R. A. Doganov, E. C.T. O'Farrell, S. P. Koenig, Y. Yeo, K. Watanabe, T. Taniguchi, A. Ziletti, A. Carvalho, D. K. Campbell, D. F. Coker, A. H. Castro Neto, and B. Oezyilmaz, arXiv: 1412.1274.
[44] I. Shirotania, Mol. Cryst. Liq. Cryst. **86**(1) (1982)